

Journal Pre-proof

Successful production of solution blow spun YBCO+Ag complex ceramics

A.L. Pessoa, M.J. Raine, D.P. Hampshire, D.K. Namburi, J.H. Durrell, R. Zadorosny

PII: S0272-8842(20)31848-4

DOI: <https://doi.org/10.1016/j.ceramint.2020.06.188>

Reference: CERI 25615

To appear in: *Ceramics International*

Received Date: 15 April 2020

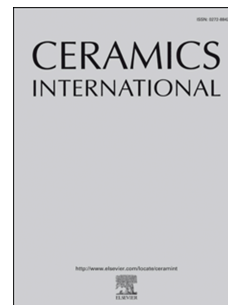
Revised Date: 21 May 2020

Accepted Date: 16 June 2020

Please cite this article as: A.L. Pessoa, M.J. Raine, D.P. Hampshire, D.K. Namburi, J.H. Durrell, R. Zadorosny, Successful production of solution blow spun YBCO+Ag complex ceramics, *Ceramics International* (2020), doi: <https://doi.org/10.1016/j.ceramint.2020.06.188>.

This is a PDF file of an article that has undergone enhancements after acceptance, such as the addition of a cover page and metadata, and formatting for readability, but it is not yet the definitive version of record. This version will undergo additional copyediting, typesetting and review before it is published in its final form, but we are providing this version to give early visibility of the article. Please note that, during the production process, errors may be discovered which could affect the content, and all legal disclaimers that apply to the journal pertain.

© 2020 Published by Elsevier Ltd.



Successful production of Solution Blow Spun YBCO+Ag complex ceramics

A. L. Pessoa^a, M. J. Raine^b, D. P. Hampshire^b, D. K. Namburi^c, J. H. Durrell^c, R. Zadorosny^{a,*}

^a*Superconductivity and Advanced Materials Group, São Paulo State University (UNESP)
Campus at Ilha Solteira, Brazil*

^b*Superconductivity Group, Centre for Materials Physics, Department of Physics, Durham
University. DH1 3LE, UK*

^c*Department of Engineering, University of Cambridge, Trumpington Street, Cambridge
CB2 1PZ, UK*

Abstract

YBCO fabrics composed of nanowires, produced by solution blow spinning (SBS) are so brittle that the Lorentz force produced by induced currents can be strong enough to damage them. On the other hand, it is known that silver addition improves the mechanical and flux pinning properties of ceramic superconductors. Thus, in this work, we show how we successfully obtained a polymeric precursor solution containing YBCO+Ag salts, which can be spun by the SBS route to produce ceramic samples. Yttrium, barium, copper, and silver metal acetates, and polyvinylpyrrolidone (PVP) (in a ratio of 5:1wt [PVP:acetates]) were dissolved in a solution with 61.5 wt% of methanol, 12 wt% of propionic acid, and 26.5 wt% of ammonium hydroxide, together with 6 wt% of PVP in solution. Three different amounts of silver (10 wt%, 20 wt%, and 30 wt%) were used in $\text{YBa}_2\text{Cu}_3\text{O}_{7-x}$. The TGA characterizations revealed a lowering of crystallization and partial melting temperatures by about 30 °C. SEM images show that after burning out the polymer, a fabric composed of nanowires of diameters up to 380 nm is produced. However, after the sintering process at 925 °C for 1 h, the nanowires shrink into a porous-like sample.

Keywords: solution blow spinning, silver addition, YBCO, sol-gel,

*

Email address: rafael.zadorosny@unesp.br (R. Zadorosny)

chemical route

1 1. Introduction

2 The main applications of superconductors are based on devices made by
3 low-temperature materials like NbTi [1] and Nb₃Sn [2]. However, since the
4 discovery of ceramic high-temperature superconductors (HTS), efforts have
5 been made to develop materials and devices with properties and forms specific
6 to each required application. The pros of using HTS in turbines, generators,
7 motors, magnetic shielding, and NMR/MRI are the reduced weight, high
8 efficiency, compact size, low noise, high trapped fields, and so on [3, 4].
9 On the other hand, the cons of using HTS are their high production cost,
10 high ac-losses, non-homogeneous trapped field distribution, and high cost
11 and reliability of the cooling systems. Some of these issues, however, can
12 be solved by producing materials following facile and low-cost routes and
13 aiming for high values of critical current density J_c and its homogeneous
14 distribution along the length of the materials. Additionally, high porous
15 superconductors, such as those produced by solution-blow spinning (SBS)
16 [5, 6], electrospinning [7, 8], and in foam-like structures [9, 10], could be used
17 to increase cooling efficiency due to their increased surface areas.

18 Particularly in the case of SBS, the samples have a fabric-like structure
19 formed by network of wires that produces a thin porous material. However,
20 as can be seen by the data in Ref. [11] the samples are very fragile; they are
21 pulverized during magnetic measurements by the Lorentz force generated by
22 the induced currents in the wires. Therefore, to study their superconduct-
23 ing properties in a wide range of fields and temperatures, it is necessary to
24 improve their mechanical properties.

25 Research works carried out on bulk (RE)BCO materials, specially in
26 YBa₂Cu₃O_{7-x} (YBCO) system, showed that both the the mechanical [12,
27 13, 14, 15] and superconducting [15, 16, 17] properties could be significantly
28 improved through addition of silver. Some of the other benefits of adding
29 silver is that it does not chemically react with YBCO [17, 18, 19], it im-
30 proves pinning sites [20], it modifies weak-links [21, 22, 23], and it enhances
31 J_c [18, 24].

32 A variety of silver composites have been added in YBCO system, such as
33 metallic Ag [18], Ag₂O [12], and AgNO₃ [13, 24]. The samples were usually
34 produced by solid-state reaction [13, 18, 24], melting-growth-like processes
35 [12], and by electrochemical routes [25]. In Ref. [26], a sol-gel chemical

36 route was used to dope the barium site by silver in the production of YBCO
37 pellets. It is reported that high concentrations of silver depreciate the super-
38 conducting properties but in small concentrations, it slightly enhances the
39 critical temperature T_c and critical current density J_c . However, as discussed
40 in Ref. [27], there is some controversy as to the extent to which Ag can be
41 doped into YBCO samples. Also, to our best knowledge, there is no infor-
42 mation about how the inclusion of silver affects the production process of
43 porous samples using chemical routes, such as in SBS.

44 The SBS technique was first reported in Ref. [28]. In such a technique,
45 polymer solutions are spun by compressed air from an inner needle up to a
46 collector [28, 29]. Along the working distance i.e. the space between the nee-
47 dle and the collector, the solvents have to evaporate, allowing the formation
48 of stretched, thin fibers with diameters of the order of hundreds of nanome-
49 ters. Thus, solutions with no water (or with very low water content) are
50 crucial to this technique to ensure that the volatility of the solution remains
51 sufficiently high. Apart from some silver composites being easily dissolved in
52 a variety of solvents (including water), the synthesis of a precursor solution
53 with Y, Ba, Cu, and Ag ions is greatly challenging. Here, we describe a
54 sol-gel-based synthesis method for obtaining fabric-like samples using SBS
55 and we present structural characterizations showing the influence of silver
56 content on those properties.

57 2. Materials and Methods

58 One-pot-like method [30] was used to synthesize the precursor solution,
59 and the reagents used are shown in Table 1. All salts are heated at 100 °C for
60 about 24 h before being weighed, ensuring that there is no moisture in the
61 salts. This is particularly important as some of these salts are hydrophilic in
62 nature.

63 2.1. Sol-gel process

64 The Y, Ba, and Cu acetates were stoichiometrically weighed in the molar
65 ratio 1:2:3, respectively. The Ag acetate was weighed in three concentrations
66 namely 10 wt%, 20 wt%, and 30 wt% with respect to the final mass of
67 ceramic YBCO. Based on the amount of acetates, PVP was weighed in the
68 ratio 5:1 (acetates:PVP). The mass of solvent was set to ensure that the
69 concentration of PVP in solution was 6 wt%. The acetates were placed
70 in a vessel in the specific order Y, Ba, Cu, and Ag, and then propionic

Reagents	Chemical formula	Purity (%)	Brand
Yttrium acetate	$C_6H_9O_{6.x}H_2O$	99.9	Sigma
Barium acetate	$C_4H_6BaO_4$	99	Sigma-Aldrich
Copper acetate	$C_4H_6CuO_4H_2O$	99	Sigma-Aldrich
Silver acetate	$C_2H_3AgO_2$	99	Sigma-Aldrich
Poli(vinylpyrrolidone)*	$(C_6H_9NO)_n$	99.99	Sigma-Aldrich
Propionic acid	$C_3H_6O_2$	99.5	Sigma-Aldrich
Methanol	CH_3OH	99.8	Vetec
Ammonium hydroxide	NH_4OH	PA	Dinamica

*PVP $1\ 300\ 000\ g\ mol^{-1}$

Table 1: List of reagents used in the synthesis of precursor solutions.

71 acid (12 wt%), methanol (61.5 wt%), and ammonium hydroxide (26.5 wt%)
 72 were added. After five minutes of stirring, the PVP was added. The final
 73 precursor solution was magnetically stirred for 24 h, with the vessel closed
 74 hermetically at room temperature (around 28 °C). Figure 1(a) shows the
 75 stabilized YBCO precursor solution and in panel (b) a loaded syringe used
 76 in the SBS apparatus. The samples studied in the present work are labeled as
 77 YAg0, YAg10, YAg20, and YAg30 with correspondence to the concentration
 78 of Ag in YBCO as 0 wt%, 10 wt%, 20 wt%, and 30 wt%, respectively.

79 2.2. Solution-blow spinning

80 A 10 ml syringe was connected to a 25G (diameter of 0.5 mm) needle.
 81 The air pressure of the compressed air cylinder was adjusted to 1 kPa and
 82 the working distance between the needle and the collector was set to 40 cm.
 83 The cylindrical collector was rotated at 40 rpm and the solution within the
 84 syringe was injected into the compressed gas airflow at a rate of $3\ ml\ h^{-1}$.
 85 A halogen light was placed above the working distance to locally heat the
 86 ejected polymer jet, evaporating the solvents prior to the jet's impact onto
 87 the rotating collector.

88 2.3. Heat-treatments

89 The as-collected sample was firstly heat-treated at 100 °C for 1 h and then
 90 at 150 °C for another 1 h with a heating rate of $5\ ^\circ C\ min^{-1}$. Some portions
 91 of that sample were then used to obtain SEM images. The polymer decom-
 92 position was carried out at 600 °C for 3 h ramping the temperature up and

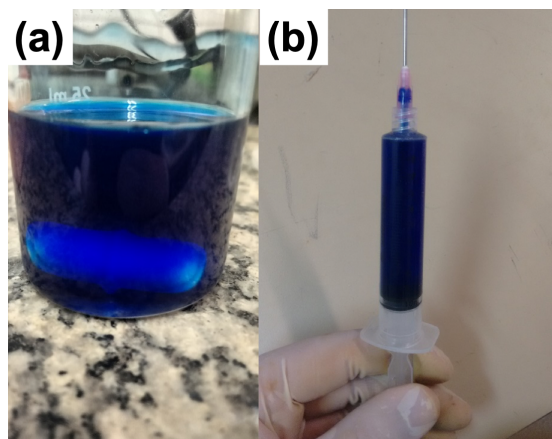


Figure 1: (a) The YAg10 precursor solution. (b) Precursor solution loaded in a 10 ml syringe used in the SBS technique.

93 down at a rate of $1\text{ }^{\circ}\text{C min}^{-1}$. Some pieces of the sample at that stage were
 94 also used to make SEM analysis. The synthesis was carried out in a tube
 95 furnace. The heat-treatment consisted of increasing the temperature from
 96 room temperature to $820\text{ }^{\circ}\text{C}$ at $3\text{ }^{\circ}\text{C min}^{-1}$ and dwelling for 14 h. Durign the
 97 heating process, flowing O_2 was turned on at $500\text{ }^{\circ}\text{C}$. After that dwell period,
 98 the temperature was increased at $1\text{ }^{\circ}\text{C min}^{-1}$ to $925\text{ }^{\circ}\text{C}$ and this was held for
 99 1 h. Then, also at $1\text{ }^{\circ}\text{C min}^{-1}$, the temperature was decreased to $725\text{ }^{\circ}\text{C}$ for
 100 6 h; then at $3\text{ }^{\circ}\text{C min}^{-1}$ to $450\text{ }^{\circ}\text{C}$ for 24 h. Finally, the O_2 gas flow was turned
 101 off and the temperature was decreased to room temperature at $3\text{ }^{\circ}\text{C min}^{-1}$.

102 2.4. Characterizations

103 Thermogravimetric measurements were carried out on the samples YAg0
 104 and YAg10 (obtained after a heat-treatment at $600\text{ }^{\circ}\text{C}$), employing TA In-
 105 strument, model SDT-Q600. Measurements were carried out under flowing
 106 compressed air at a rate of 100 ml min^{-1} and the temperature was increased
 107 from $25\text{ }^{\circ}\text{C}$ to $1000\text{ }^{\circ}\text{C}$ at a rate of $10\text{ }^{\circ}\text{C min}^{-1}$. For the scanning electron mi-
 108 croscopy (SEM) measurements, an EVO LS15 Zeiss operated at 20 kV was
 109 used. For that, the samples were attached in an aluminum sample holder with
 110 carbon tape, and gold was sputtered on their surface for 2 min (5 nm average
 111 thickness) using a QUORUM Model Q150T E. The diameter distribution was
 112 measured using a randomly selected set of 100 wires and the free software
 113 package ImageJ. The x-ray analysis (XRD) was performed in a Shimadzu
 114 XDR-6000 diffractometer with $\text{CuK}\alpha$ radiation (wavelength: 1.5418 \AA). The

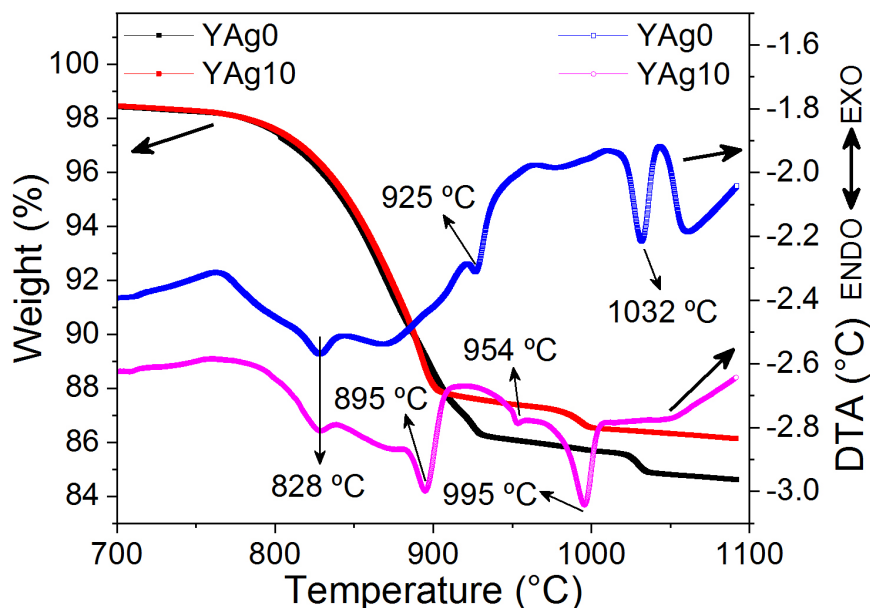


Figure 2: TG and DTA of samples YAg0 and YAg10 carried out after a heat-treatment at 600 °C. The YAg10 lost less mass due to the silver addition. From DTA curves, it is noted that the silver addition shifted the YBCO crystallization peak from 925 °C (YAg0) to 895 °C (YAg10). The partial melting peak is also shifted from 1032 °C for YAg0 to 995 °C for YAg10. The peak at 954 °C is related with the melting of metallic silver.

115 displacement ranged from $2\theta = 5^\circ$ to 60° at a scan rate of 1°min^{-1} and
 116 measuring in steps of 0.02° .

117 3. Results and Discussions

118 Thermal analysis was carried out on two samples YAg0 and YAg10, after
 119 both were heat treated at 650°C . About 15 mg of each sample was used for
 120 the measurement and the data obtained is shown in Figure 2. Both the
 121 samples exhibited a similar weight loss, as can be seen from the curves in
 122 Figure 2. The mass lost between 25°C and 700°C (not shown in Figure 2),
 123 was 1.5 %, and can be associated to the evaporation of water adsorbed in
 124 the surface of the samples from the atmosphere or even some organic groups
 125 remaining after the heat-treatment. It is also observed that YAg10 lost about
 126 1.1% less mass than YAg0 due to silver addition. It is not shown here, but it
 127 is worth pointing out that the PVP degradation occurs between 400°C and
 128 550°C [8, 31, 32].

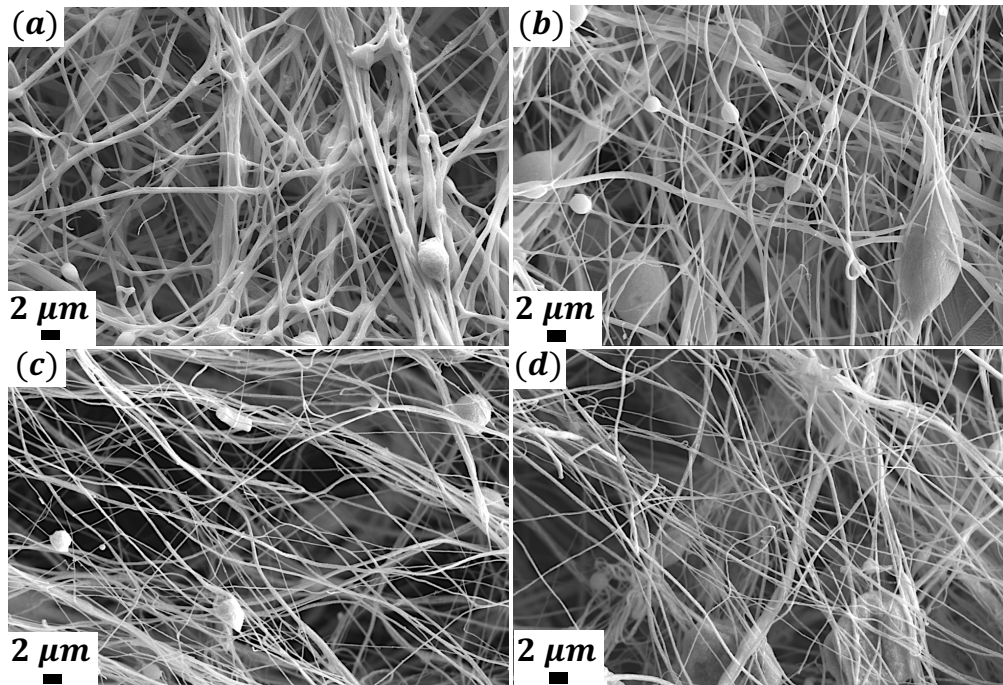


Figure 3: SEM images of samples (a) YAg0, (b) YAg10, (c) YAg20, and (d) YAg30 after calcination at 600 °C. At this step, all samples have the fabric-like morphology with beads distributed along their lengths.

129 The DTA curves of YAg0 and YAg10 are quite distinct. Both samples
 130 present an endothermic peak at 828 °C which can be associated with the
 131 reaction between $Y_2Cu_2O_5$ and $BaCuO_2$ forming YBCO [33, 34]. The en-
 132 dothermic peak at 925 °C for YAg0 can be associated with the YBCO crys-
 133 tallization, and it was the temperature chosen to be applied in all samples
 134 presented in this study. However, it can be noted that the YBCO begins to
 135 crystallize at about 895 °C for YAg10, which means that the silver addition
 136 reduced the the crystallization temperature by 30 °C (or 3%). The peak at
 137 954 °C presented by YAg10 is associated with the melting of metallic silver
 138 [35]. On the other hand, the endothermic peak at 1031 °C for YAg0 is due
 139 to a partial melting of YBCO and such a peak is shifted to 995 °C (or 3.5%)
 140 for YAg10, showing that the silver addition also decreases this temperature
 141 [14, 36, 37].

142 Based on the thermogravimetric analysis of Figure 2 and on the literature
 143 [5, 8, 31, 32], the samples were firstly heat-treated at 600 °C to ensure the

Sample	d_{av} (nm)	Deviation (nm)
YAg0	233	77
YAg10	180	68
YAg20	206	76
YAg30	191	63

Table 2: Average diameters of the samples heat-treated at 600° with their respective deviations.

144 total decomposition of the PVP. Figure 3 shows SEM images of the produced
 145 samples. All of which present a fabric-like structure with randomly entangled
 146 wires, however, it can be seen that beads are distributed along those wires.
 147 This is probably due to water from the acid–base reaction in the precursor
 148 solution synthesis. Besides that, the wires are long and smooth. Table 2
 149 shows the average diameter (d_{av}) of the samples. Wires in the size range
 150 180 nm to 233 nm were found in the samples. No clear relationship was
 151 found between d_{av} and the content of silver present in the system.

152 After the sintering process at 925 °C, the silver samples shrank, produc-
 153 ing a granular porous-like structure. The shrinkage of the samples is shown
 154 in Figure 4 (a) and (b). The scale bars within those images are an ap-
 155 proximation for comparison purposes. Figure 4(c) shows that, while the
 156 Ag-free sample YAg0 maintains its fiber-like structure, the Ag–added sam-
 157 ples showed considerable enhancement in density, as shown in Figure 4 from
 158 panels (d) to (f). With the wires closer to each other, the grains begin to
 159 coalesce during the sintering process and the samples acquire a porous-like
 160 morphology. Some works report that the heat-treatment temperatures can
 161 be reduced with Ag addition in YBCO bulks [14, 36, 37] due to enhanced
 162 heat diffusion. In the case of the present work, the presence of Ag facilitates
 163 improved heat-diffusion between the ceramic grains, decreasing the sintering
 164 temperature of the samples.

165 Figure 5 shows XRD diffractograms of all the samples currently studied
 166 where it can be seen that the BaCuO₂ phase is present within each of them.
 167 Since samples that were produced using PVP of 360 000 g mol⁻¹ instead of
 168 1 300 000 g mol⁻¹ contain a pure phase [5], we believe that a longer polymer
 169 chain could influence the ceramic phase formation. Such a study will be
 170 published in future. As the silver content increases, the intensity of the silver
 171 peaks (at around 38° and 49°) also increases. The most intense YBCO peak

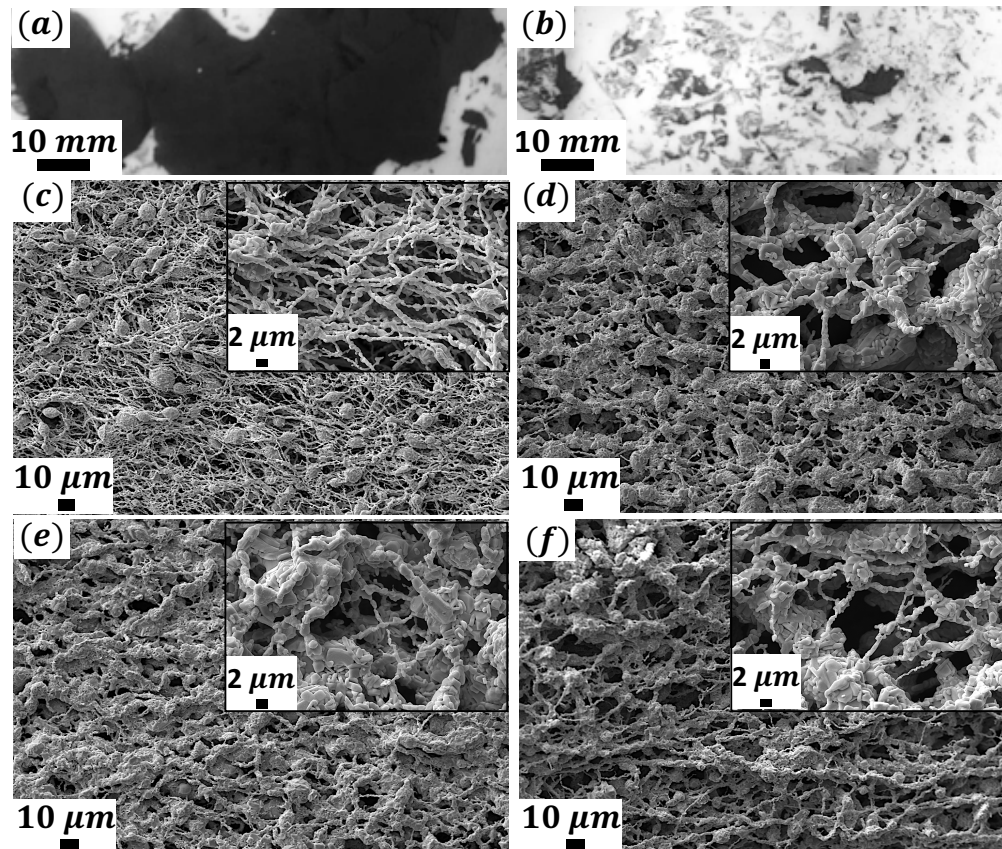


Figure 4: (a) Image of the YBCO-Ag after heat-treatment at 600 °C, and panel (b) shows the visible shrinkage of the sample after sintering at 925 °C. (c) SEM images of YAg0 sample showing the formation of the wires network structure. From (d) to (f) are the SEM images of the YAg10, YAg20, and YAg30, respectively, showing a porous-like structure due to shrinkage after the sintering process.

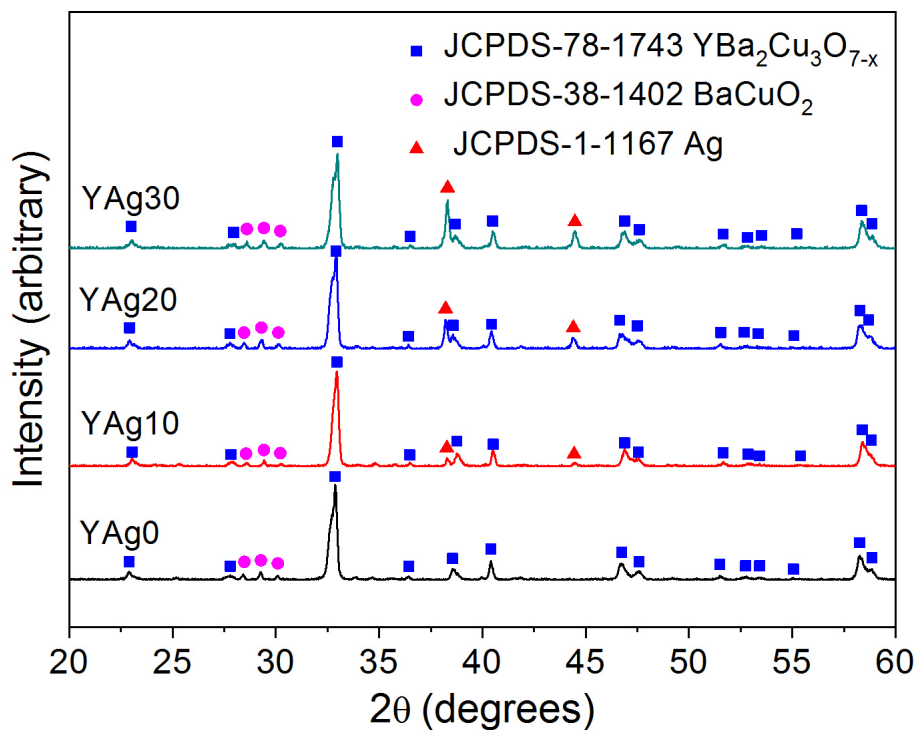


Figure 5: XRD diffractograms of the produced samples. It can be seen that BaCuO_2 is present in all the samples. The main YBCO peak is at $2\theta = 32.88^\circ$, 32.96° , 32.92° , and 32.98° , for YAg0, YAg10, YAg20, and YAg30, respectively. The metallic silver peaks are those ones at 38.28° and 44.5° for YAg10, 38.22° and 44.4° for YAg20, and 38.3° and 44.48° for YAg30.

172 position shifts with the silver addition, being at $2\theta = 32.88^\circ$, 32.96° , 32.92° ,
 173 and 32.98° , for YAg0, YAg10, YAg20, and YAg30, respectively. This can
 174 indicate that there is some saturation for silver doping above which metallic
 175 silver begins to form along the sample [27]. The peaks around $2\theta = 38.3^\circ$ and
 176 44.5° were identified as characteristic of metallic silver, and their intensity
 177 increases with increasing Ag content.

178 4. Conclusions

179 In the present work we report the synthesis of YBCO-Ag nanowires via
 180 solution blow spinning SBS technique. This approach is based on an acetate
 181 chemical route where yttrium, barium, copper and silver acetates were dis-
 182 solved in a solution with propionic acid (12 wt%), methanol (61.5 wt%),

183 and ammonium hydroxide (26.5 wt%). The silver was added in amounts
184 of 10 wt%, 20 wt%, and 30 wt%. Thermogravimetric analysis show that
185 the addition of silver decreases both the YBCO crystallization and the par-
186 tial melting temperatures by 30 °C. Both DTA and XRD characterizations
187 showed the presence of metallic silver. Another interesting influence of silver
188 in such complex ceramics is the huge densification of the samples sintered at
189 925 °C for one hour. SEM images show that the fabric-like morphology of the
190 samples heat-treated at 600 °C is lost with the sintering process, for which
191 a porous-like morphology takes place due to a shrinkage of the ceramic wire
192 network. Thus, the routine described in this study could be used to produce
193 high density bulk superconductors for use in applications such as flywheels,
194 trapped magnets, motors and generators.

195 5. Acknowledgements

196 A. L. Pessoa, R. Zadorosny, M. Raine and D. P. Hampshire acknowl-
197 edge the Brazilian agencies São Paulo Research Foundation (FAPESP, grant
198 2017/50382-8), Coordenação de Aperfeiçoamento de Pessoal de Nível Supe-
199 rior (CAPES) – Finance Code 001, and National Council of Scientific and
200 Technologic Development (CNPq, grant 302564/2018-7). We also thanks
201 Prof. Agda E. S. Albas and Silvio R. Teixeira, from UNESP-Presidente Pru-
202 dente, for the thermogravimetric measurements.

203 6. Additional information

204 ALP: orcid= 0000-0002-7949-4626, credit: Investigation, Data curation,
205 Writing - Original Draft;

206 MJR: orcid= 0000-0001-6566-6039, credit: Investigation, Data curation,
207 Writing - Original Draft, Writing - Review and Editing, Validation;

208 DPH: orcid= 0000-0001-8552-8514, credit: Conceptualization of this study,
209 Methodology, Resources, Writing - Review and Editing, Supervision, Project
210 administration, Funding acquisition;

211 DKN orcid= 0000-0003-3219-2708, credit: Data curation, Writing - Re-
212 view And Editing, Validation;

213 JHD: orcid= 0000-0003-0712-3102, credit: Writing - Review and Editing,
214 Supervision, Validation;

215 RZ: orcid= 0000-0002-2419-2049, credit: Conceptualization of this study,
216 Methodology, Resources, Writing - Original Draft, Supervision, Project ad-
217 ministration, Funding acquisition.

- 218 [1] K. M. Schaubel, A. R. Langhorn, W. P. Creedon, N. W. Johanson,
219 S. Sheynin, R. J. Thome, Development of a superconducting magnet
220 system for the ONR/GA homopolar motor, AIP Conf. Proc. 823 (2006)
221 1819, DOI: 10.1063/1.2202611
- 222 [2] K. S. Haran, D. Loder, T. O. Deppen, L. Zheng, Actively shielded, high
223 field air-core superconducting machines, IEEE Trans. Appl. Supercond.
224 26 (2016) 98–105. DOI: 10.1109/TASC.2016.2519409
- 225 [3] K. S. Haran, S. Kalsi, T. Arndt, H. Karmaker, R. Badcock, B. Buck-
226 ley, T. Haugan, M. Izumi, D. Loder, J. W. Bray, P. Masson, E.
227 W. Stautner, High power density superconducting rotating machines-
228 development status and technology roadmap, Supercond. Sci. Technol.
229 30 (2017) 123002. DOI: 10.1088/1361-6668/aa833e
- 230 [4] J. H. Durrell, M. D. Ainslie, D. Zhou, P. Vanderbemden, T. Bradshaw,
231 S. Speller, M. Filipenko, and D. A. Cardwell, Bulk superconductors:
232 a roadmap to applications, Supercond. Sci. Technol. 31 (2018) 103501.
233 DOI: 10.1088/1361-6668/aad7ce
- 234 [5] M. Rotta, L. Zadorosny, C. L. Carvalho, J. A. Malmonge, L. F. Mal-
235 monge, R. Zadorosny, YBCO ceramic nanofibers obtained by the new
236 technique of solution blow spinning, Ceramics International 42 (2016)
237 16230–16234. DOI: 10.1016/j.ceramint.2016.07.152
- 238 [6] M. Rotta, M. Motta, A. L. Pessoa, C. L. Carvalho, W. A. Ortiz, R.
239 Zadorosny, Solution blow spinning control of morphology and produc-
240 tion rate of complex superconducting $YBa_2Cu_3O_{7-x}$ nanowires, Jour-
241 nal of Materials Science: Materials in Electronics 30 (2019) 9045–9050.
242 DOI: 10.1007/s10854-019-01236-w
- 243 [7] X. L. Zeng, M. R. Koblishka, T. Karwoth, T. Hauet, U. Hartmann,
244 Preparation of granular Bi-2212 nanowires by electrospinning, Super-
245 cond. Sci. Technol. 30 (2017) 035014. DOI: 10.1088/1361-6668/aa544a
- 246 [8] Z. Shen, Y. Wang, W. Chen, L. Fei, K. Li, H. L. W. Chan, L. Bing,
247 Electrospinning preparation and high-temperature superconductivity
248 of $YBa_2Cu_3O_{7-x}$ nanotubes. Journal of Materials Science 48 (2013)
249 3985–3990. DOI: 10.1007/s10853-013-7207-y

- 250 [9] E. S. Reddy, G. J. Schmitz, Superconducting foams, *Supercond. Sci.*
251 *Technol.* 15 (2002) L21–L24. DOI: 10.1088/0953-2048/15/8/101
- 252 [10] M. R. Koblishka, S. P. K. Naik, A. Koblishka-Veneva, M. Murakami,
253 D. Gokhfeld, E. S. Reddy, G. J. Schmitz, Superconducting YBCO
254 Foams as Trapped Field Magnets. Preprints 2019, 2019010174 (doi:
255 10.20944/preprints201901.0174.v1).
- 256 [11] Data showing non-reproducibility measurements of fabric-like YBCO
257 samples due to its pulverization by the induced Lorentz force in
258 the brittle wires, <https://dx.doi.org/10.15128/r2f1881k89x> and as-
259 sociated materials are on the Durham Research Online website:
260 <http://dro.dur.ac.uk/>
- 261 [12] P. Diko, G. Fuchs, G. Krabbes, Influence of silver addition on cracking in
262 melt-grown YBCO, *Physica C: Superconductivity and its Applications*
263 363 (2001) 60–66. DOI: 10.1016/S0921-4534(01)00622-0
- 264 [13] E. Mogilko, Y. Schlesinger, The $AgNO_3$ route to the YBCO/Ag com-
265 posite: Structural and electrical properties. *Supercond. Sci. Technol.* 10
266 (1997) 134–141. DOI: 10.1088/0953-2048/10/3/003
- 267 [14] J. V. J. Congreve, Y. Shi, K. Y. Huang, A. R. Dennis, J. H. Dur-
268 rell, D. A. Cardwell, Improving Mechanical Strength of YBCO Bulk
269 Superconductors by Addition of Ag, *IEEE Transactions on Applied Su-
270 perconductivity* 29 (2019) 6802305. DOI: 10.1109/TASC.2019.2907474
- 271 [15] P. D. Azambuja, P. R. Júnior, A. R. Jurelo, F. C. Serbena, C.
272 E. Foerster, R. M. Costa, G. B. Souza, C. M. Lepienski, A. L.
273 Chinelatto, Effects of Ag addition on some physical properties of gran-
274 ular $YBa_2Cu_3O_{7-\delta}$ superconductor, *Braz. J. Phys.* 39 (2009), pp.
275 638–644. DOI: 10.1590/S0103-97332009000600005
- 276 [16] B. A. Malik, M. A. Malik, K. Asokan, Magneto transport study of
277 YBCO: Ag composites. *Current Applied Physics* 16 (2016) 1270–1276.
278 DOI: 10.1016/j.cap.2016.07.004
- 279 [17] N. D. Kumar, P. M. S. Raju, S. P. K. Naik, T. Rajasekha-
280 ran, V. Seshubai, Effect of Ag addition on the microstructures and
281 superconducting properties of bulk YBCO fabricated by direction-
282 ally solidified preform optimized infiltration growth process. *Physica*

- 283 C: Superconductivity and its Applications 496 (2014) 18–22. DOI:
284 10.1016/j.physc.2013.06.013
- 285 [18] B. A. Malik, M. A. Malik, K. Asokan, Enhancement of the critical cur-
286 rent density in YBCO/Ag composites. Chinese Journal of Physics 55
287 (2017) 170–175. DOI: 10.1016/j.cjph.2016.10.015
- 288 [19] H. Azhan, F. Fariesha, S. Y. S. Yusainee, K. Azman, S. Khalida,
289 Superconducting properties of Ag and Sb substitution on low-density
290 $YBa_2Cu_3O_\delta$ superconductor. Journal of Superconductivity and Novel
291 Magnetism 26 (2013) 931–935. DOI: 10.1007/s10948-012-2020-4
- 292 [20] S. V. Pysarenko, A. V. Pan, S. X. Dou, Influence of Ag-
293 doping and thickness on superconducting properties of $YBa_2Cu_3O_7$
294 films. Physica C: Superconductivity 460 (2007) 1363–1364. DOI:
295 10.1016/j.physc.2007.04.175
- 296 [21] H. Salamati, A. A. Babaei-Brojeny, M. Safa, Investigation of weak links
297 and the role of silver addition on YBCO superconductors. Supercond.
298 Sci. Technol. 14 (2001) 816–819. DOI: 10.1088/0953-2048/14/10/302
- 299 [22] P. Rani, A. Pal, V. P. S. Awana, High field magneto-transport study of
300 $YBa_2Cu_3O_{7-x}Ag_x$ ($x = 0.00 - 0.20$). Physica C. Superconductivity and
301 its Applications 497 (2014) 19–23. DOI: 10.1016/j.physc.2013.10.008
- 302 [23] M. Tepe, I. Avci, H. Kocoglu, D. Abukay, Investigation of the variation in
303 weak-link profile of $YBa_2Cu_{3-x}Ag_xO_{7-\delta}$ superconductors by Ag doping
304 concentration. Solid State Communications 131 (2004) 319–323. DOI:
305 10.1016/j.ssc.2004.05.015
- 306 [24] M. Farbod, M. R. Batvandi, Doping effect of Ag nanoparticles on
307 critical current of $YBa_2Cu_3O_{7-\delta}$ bulk superconductor. Physica C:
308 Superconductivity and its Applications 471 (2011) 112–117. DOI:
309 10.1016/j.physc.2010.11.005
- 310 [25] S. Reich, I. Felner, Nonrandom ceramic superconductor-metal com-
311 posites. Journal of Applied Physics 67 (1990) 388–392. DOI:
312 10.1063/1.345267

- 313 [26] F. F. Ramli, N. A. Wahab, A. Hashim, Microstructure and supercon-
314 ducting properties of Ag-substituted $YBa_{2-x}Ag_xCu_3O_{7-\delta}$ ceramics pre-
315 pared by sol-gel method. MJFAS Malaysian Journal of Fundamental and
316 applied sciences 13 (2017) 82–85. DOI: 10.11113/mjfas.v13n2.655
- 317 [27] J. M. S. Skakle, Crystal chemical substitutions and doping of
318 $YBa_2Cu_3O_x$ and related superconductors, Materials Science and En-
319 gineering R23 (1998) 1–40. DOI: 10.1016/S0927-796X(98)00010-2
- 320 [28] E. S. Medeiros, G. M. Glenn, A. P. Klamczynski, W. J. Orts, L. H.
321 C. Mattoso, Solution blow spinning: a new method to produce micro-
322 and nanofibers from polymer solutions, J. Appl.Polym.Sci. 113 (2009)
323 2322–2330. DOI: 10.1002/app.30275
- 324 [29] J. L. Daristotle, A. M. Behrens, A. D. Sandler, P. Kofinas, A review
325 of the fundamental principles and applications of solution blow spin-
326 ning. Appl. Mater. Interfaces 8 (2016) 34951–34963. DOI: 10.1021/ac-
327 sami.6b12994
- 328 [30] M. Rotta, M. Motta, A. L. Pessoa, C. L. Carvalho, C. V. Deimling, P.
329 N. Lisboa-Filho, W. A. Ortiz, R. Zadorosny, One-pot-like facile synthe-
330 sis of $YBa_2Cu_3O_{7-\delta}$ superconducting ceramic: Using PVP to obtain a
331 precursor solution in two steps, Materials Chemistry and Physics 243
332 (2020) 122607. DOI: 10.1016/j.matchemphys.2019.122607
- 333 [31] J. Yuh, L. Perez, W. M. Sigmund, J. C. Nino, Sol-gel based synthesis
334 of complex oxide nanofibers, J.Sol-GelSci. Technol. 42 (2007) 323–329.
335 DOI: 10.1007/s10971-007-0736-6
- 336 [32] E. A. Duarte, N. G. Rudawski, P. A. Quintero, M. W. Meisel, J.
337 C. Nino, Electrospinning of superconducting YBCO nanowires, Su-
338 percond. Sci. Technol. 28 (2014) 015006–015012. DOI: 10.1088/0953-
339 2048/28/1/015006
- 340 [33] L. C. Pathak, S. K. Mishra, A review on the synthesis of
341 Y–Ba–Cu–oxide powder, Supercond. Sci. Technol. 18 (2005)
342 R67–R89. DOI: 10.1088/0953-2048/18/9/R01
- 343 [34] N. A. Kalanda, V. M. Trukhan, S. F. Marenkin, Phase Transforma-
344 tions in the $Y_2Cu_2O_5$ – $BaCuO_2$ System, Inorganic Materials 38 (2002)
345 494–497.

- 346 [35] S. Kohayashi, S. Yoshizawa, H. Miyairi, H. Nakane, S. Nagaya, Large
347 domain growth of Ag-doped YBaCuO-system superconductor, Materials
348 Science and Engineering: B 53 (1998) 70–74. DOI 10.1016/S0921-
349 5107(97)00304-8
- 350 [36] Y. Nakamura, K. Tachibana, H. Fujimoto, Dispersion of silver in the
351 melt grown $YBa_2Cu_3O_{6+x}$ crystal, Physica C 306 (1998) 259–270. DOI:
352 10.1016/S0921-4534(98)00368-2
- 353 [37] C. Cai, K. Tachibana, H. Fujimoto, Study on single-domain growth
354 of $Y_{1.8}Ba_{2.4}Cu_{3.4}O_y/Ag$ system by using $Nd123/MgO$ thin film as
355 seed, Supercond. Sci. Technol. 13 (2000) 698–702. DOI: 10.1088/0953-
356 2048/13/6/314

Declaration of interests

The authors declare that they have no known competing financial interests or personal relationships that could have appeared to influence the work reported in this paper.

The authors declare the following financial interests/personal relationships which may be considered as potential competing interests:

On behalf the authors,

Prof. Dr. Rafael Zadorosny

Universidade Estadual Paulista - UNESP

Departamento de Física e Química

Phone: +55 18 3743-1903 Fax: +55 18 3742-4868; e-mail: rafael.zadorosny@unesp.br



Journal Pre-proof